ISSN 1028-334X, Doklady Earth Sciences, 2020, Vol. 490, Part 1, pp. 23–27. © Pleiades Publishing, Ltd., 2020.
Russian Text © The Author(s), 2020, published in Doklady Rossiiskoi Akademii Nauk. Nauki o Zemle, 2020, Vol. 490, No. 1, pp. 27–32.

GEOPHYSICS

Model Estimates of Global and Regional Climate Changes in the Holocene

Academician I. I. Mokhov[a,b,c], A. V. Eliseev[a,b,d,*], and V. V. Guryanov[d]

Received October 14, 2019; revised October 14, 2019; accepted October 18, 2019

Abstract—On the basis of simulations using a global climate model, the global and regional climate changes in the Holocene are estimated. According to our results, the average contemporary level of global near-surface temperature in recent decades exceeded the respective values during the last 10 kyr, including the period of the Holocene optimum (Middle Holocene, about 6 kyr B.P.). However, modern temperature regimes in particular regions (e.g., Europe) may be below the maximum warming level of the Middle Holocene. Global and regional climate changes and variations in the carbon cycle characteristics over the last century (based on model calculations, with the anthropogenic effect being taken into account) considerably differ from the variations in the preceding centuries and millennia, when natural impacts on the climate system played the key role.

Keywords: Holocene, climate changes, simulation, IAP RAS CM

DOI: 10.1134/S1028334X20010067

On the basis of simulations using a global climate model, we estimated the global and regional climate changes in the Holocene. According to our results, the average contemporary level of global near-surface temperature in recent decades exceeded the respective values during the last 10 kyr, including the period of the so-called Holocene optimum (in other words, Middle Holocene, about 6 kyr B.P.). However, the modern temperature regimes in particular regions (e.g., Europe) may be below the maximum warming level of the Middle Holocene. Global and regional climate changes and variations in the characteristics of the carbon cycle over the last century (based on the model calculations, with the anthropogenic effect being taken into account) differ considerably from the variations of the preceding centuries and millennia, when the natural impacts on the climate system, including the changes in the orbital parameters of the Earth's rotation around the Sun and solar activity, played the key role.

For estimating global and regional climate changes during the last 10 kyr in the Holocene, we performed numerical calculations using the global climate model developed in the Obukhov Institute of Atmospheric Physics, Russian Academy of Sciences (IAP RAS CM) [1–4]. Numerical calculations using the IAP RAS CM were made taking into account parameters such as changes in the orbital parameters of the Earth [5], total solar irradiance, the optical thickness of stratospheric (volcanic) aerosols (only for 501–2000 AD), the concentrations of greenhouse gases (CO_2, CH_4, and N_2O) in the atmosphere, areas of pastures and croplands, and population density. When taking into account the changes in the sulfate aerosol content in the troposphere, we assumed that its level in the mid-19th century characterized the distribution of natural sulfates for the entire Holocene. The data used are presented in more detail in Table 1.

Variations in the near-surface temperature during the 20th century are generally adequately reproduced by calculations using the IAP RAS CM. Remarkably, interannual and interdecadal variability appears to be underestimated (Fig. 1b), which is characteristic of the modern climate models of intermediate complexity, to which the IAP RAS CM belongs [1–4]. According to calculations using the IAP RAS CM, the global near-surface temperature increased during the 20th century by 0.6°C, which is quite close to the estimated value of 0.7°C obtained by the data of HadCRUT4 (www.cru.uea.ac.uk/data). The difference between these two estimates, obtained by model calculations and from real observations, can be attributed to natural variability.

In Fig. 1a, the results of model simulations of how global near-surface temperature changes in the Holocene are presented. According to calculations using the IAP RAS CM, the values of global surface air tem-

[a] *Obukhov Institute of Atmospheric Physics, Russian Academy of Sciences, Moscow, 119017 Russia*
[b] *Lomonosov Moscow State University, Moscow, 119991 Russia*
[c] *Moscow Institute of Physics and Technology, Dolgoprudnyi, Moscow oblast, 141701 Russia*
[d] *Kazan (Volga Region) Federal University, Kazan, 420008 Russia*
**e-mail: eliseev@ifaran.ru*

Table 1. Data on the external effects on the Earth system, used in numerical calculations in the CM IAP RAS

Variable	Data source
Total solar irradiance	https://www1.ncdc.noaa.gov/pub/data/paleo/climate_forcing/solar_variability/steinhilber2009tsi.txt
Optical thickness of volcanic aerosols in the stratosphere	For 501–2000 AD, https://www1.ncdc.noaa.gov/pub/data/paleo/climate_forcing/volcanic_aerosols/gao2008ivi2/IVI2LoadingLatHeight501-2000_Version2_Oct2012.txt; the data before 500 AD are not considered
CO_2 content in the atmosphere	For 10–2 kyr B.P., https://www1.ncdc.noaa.gov/pub/data/paleo/icecore/antarctica/antarctica2015co2.xls; For 2–0 kyr B.P., https://www.geosci-model-dev.net/10/2057/2017/gmd-10-2057-2017-supplement.zip
CH_4 content in the atmosphere	For 10–2 kyr B.P., average of two sources (https://www1.ncdc.noaa.gov/pub/data/paleo/icecore/antarctica/epica_domec/dc_ch4_hol_fl02.txt, https://www1.ncdc.noaa.gov/pub/data/paleo/icecore/greenland/summit/grip/gases/gripch4.txt) is taken; for 2–0 kyr B.P., https://www.geosci-model-dev.net/10/2057/2017/gmd-10-2057-2017-supplement.zip
N_2O content in the atmosphere	For 2–0 kyr B.P., https://www1.ncdc.noaa.gov/pub/data/paleo/icecore/greenland/summit/gisp2/gases/gisp2_n2o.txt; for 2–0 kyr B.P., https://www.geosci-model-dev.net/10/2057/2017/gmd-10-2057-2017-supplement.zip
Concentration of sulfate aerosols in the troposphere	For 1850–2000 AD, https://tntcat.iiasa.ac.at/RcpDb/download/Aerosols/; before 1850 AD content is assumed to be constant
Areas of crops and pastures	HYDE-3.2 (ftp://ftp.pbl.nl/hyde/hyde3.2/baseline)
Population density	HYDE-3.2 (ftp://ftp.pbl.nl/hyde/hyde3.2/baseline)

perature in recent decades and in the last 100 years are, on the whole, noticeably higher than in the previous centuries and millennia of the Holocene. It should be noted that no remarkable increase in surface air temperature is observed on a global scale during the Holocene optimum (in the mid-Holocene). This is consistent with the contemporary paleoreconstructions [6, 7] and other calculations using climate models [7]. The temperatures obtained by calculations using the IAP RAS CM can be corrected, in particular, when taking into consideration the shifts of vegetation zones. Nevertheless, the model is qualitatively and quantitatively correct in reproducing the latitude dependence of variations in surface air temperature

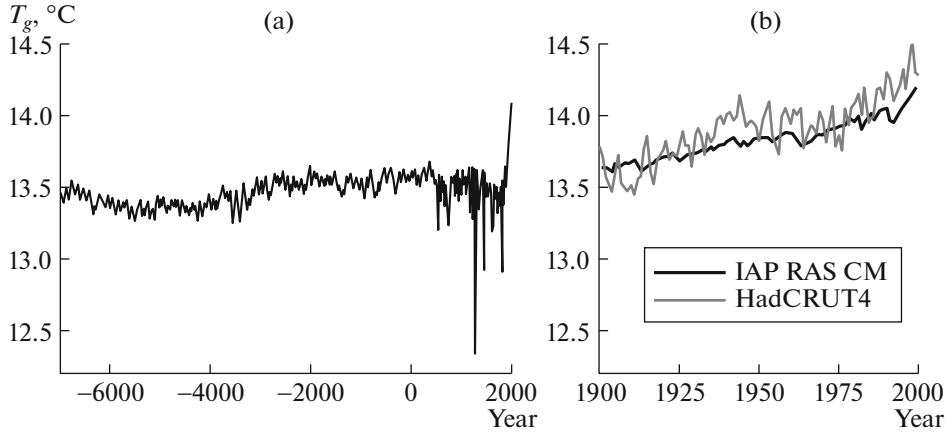

Fig. 1. Variations in the global surface air temperature (°C) in the Holocene (a) and in the 20th century alone (b), based on the model calculations (left), in comparison with the HadCRUT4 data.

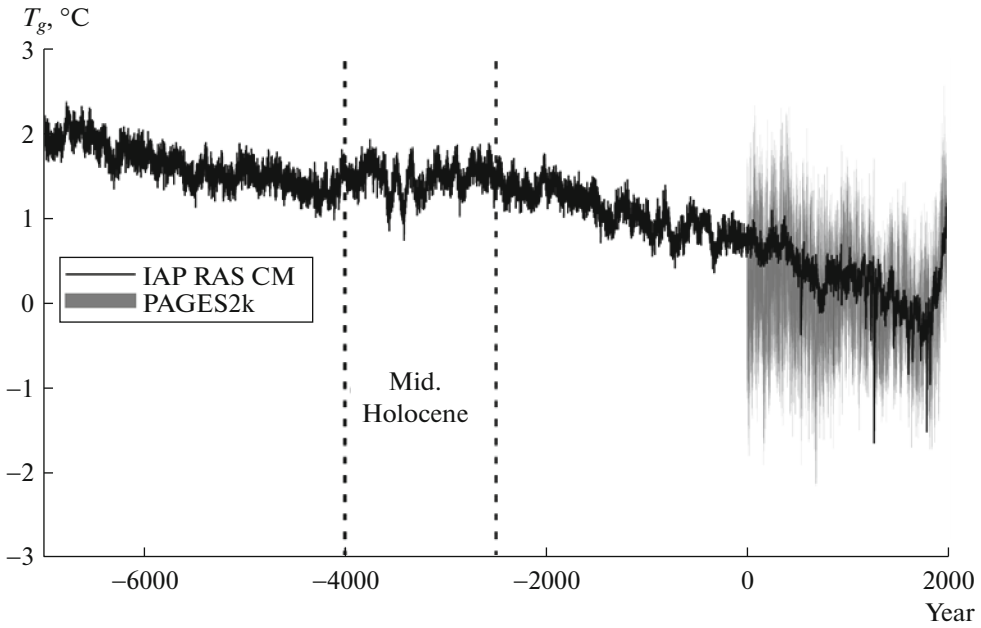

Fig. 2. Variations in summer surface air temperature (°C) for the region of Europe (35°–70° N, 10°–40° E) based on model calculations in comparison with the reconstructions by PAGES2k. The temperature anomalies relative to the average summer surface air temperature for 1500–2000 AD are shown. Vertical dashed lines mark the Middle Holocene interval of 6–4.5 kyr B.P.

above land in the Northern Hemisphere during the Holocene up until the beginning of the Little Ice Age, obtained in [6] (Fig. 3).

Although a significant global-scale increase in temperature is absent during the Holocene optimum, there are regional-scale temperature peaks during the Middle and Early Holocene, in particular, those in summer for some parts of Europe (Fig. 2). According to calculations using the IAP RAS CM, the long-period regional variations in surface air temperature during the last two millennia generally follow those after the PAGES2k reconstructions (PastGlobalChanges, the 2kNetwork; http://pastglobalchanges.org/science/wg/2k-network/data).

According to Fig. 2, the model-based values of the surface air summer temperature in the region of Europe (35°–70° N; 10°–40° E), which have rapidly grown in the last century, by the end of the 20th century approached their Middle Holocene maxima (6–4.5 kyr B.P.). On the global scale, the model-based surface air temperature in the 20th century considerably exceeded the maximal values of 6–4.5 kyr B.P. (Fig. 1). This is related to the significant spatial heterogeneity of climate changes with significant differences for various seasons.

Figure 3 demonstrates the model-based latitude–longitude changes in the annual mean surface air temperature during the Middle Holocene relative to the last 30 years of the 20th century. According to the model calculations, the mean surface air temperatures in most regions of the Earth by the end of the 20th century exceeded the respective Middle Holocene values; the only exceptions were the arctic lati-

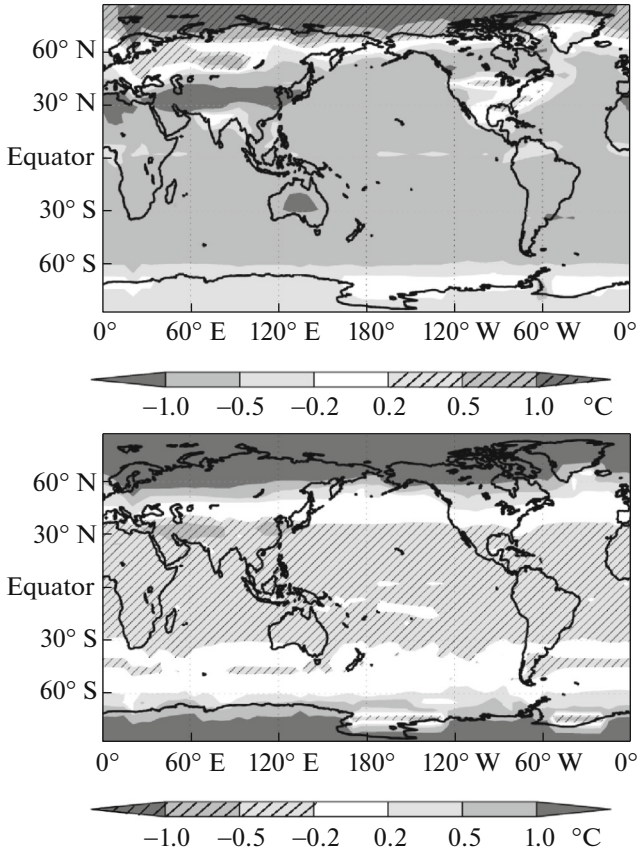

Fig. 3. Variations in the annual mean surface air temperature (°C) in the Middle Holocene (6–4.5 kyr B.P.) relative to 1970–1999 (top panel) and for the period from 9 kyr B.P. until 1500 AD, based on calculations using IAP RAS CM.

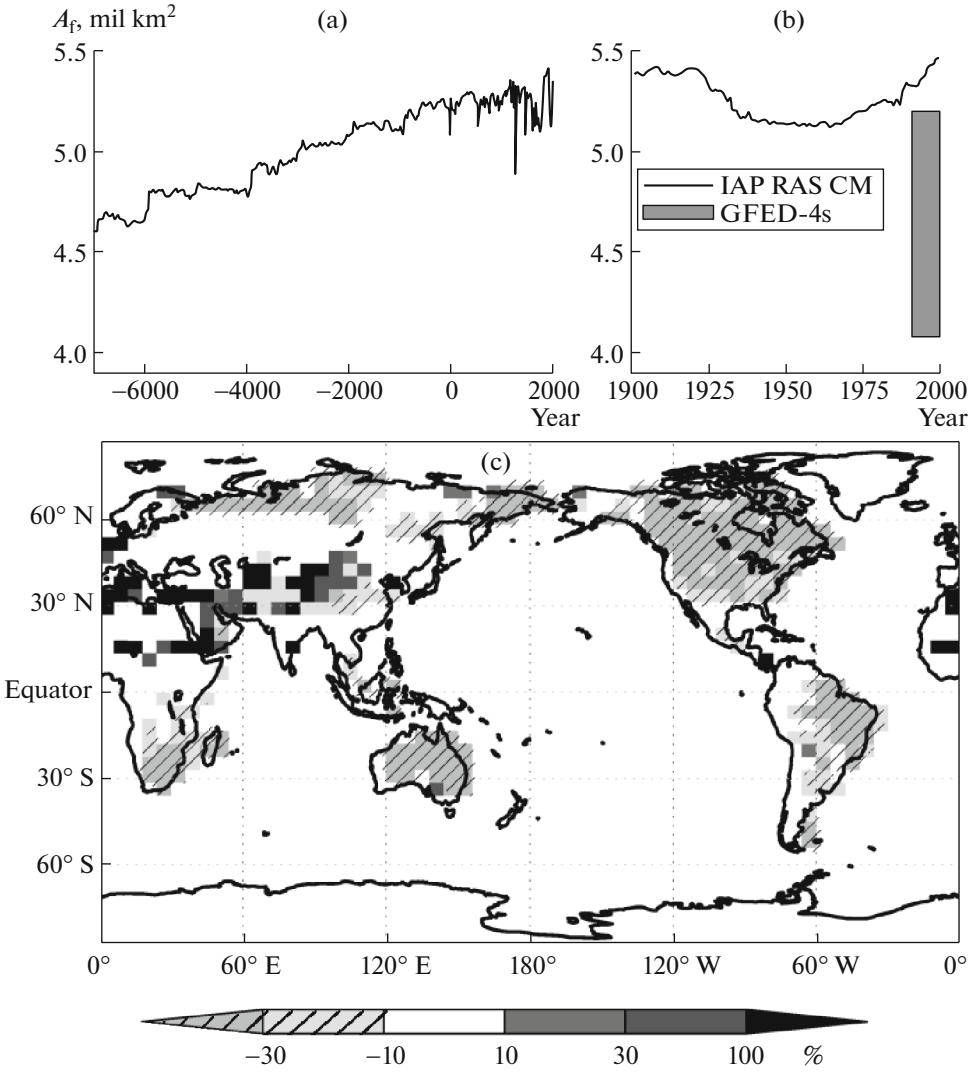

Fig. 4. Variations in global area of natural fires (A_f, mil km^2) in the Holocene (a) and for the 20th century alone (b), based on the model calculations in comparison with the uncertainty range from the GFED4 data for the period of 2001–2010. The bottom panel (c) illustrates the changes in area under fires in the period of 6–4.5 kyr B.P. (in %, relative to 1970–1999 AD).

tudes, relatively large regions in North Eurasia, and mid-latitude and subtropical regions of North America. In particular, by the end of the 20th century, the model-based surface air temperatures in the subpolar and middle latitudes of Eurasia were higher than the respective Middle Holocene values in summer but lower than those in winter. The model results demonstrate considerable differences between Eurasia and North America. It should be noted that the Middle Holocene climate changes relative to the late-20th century winter temperatures, estimated using the IAP RAS CM, are close to the estimates obtained in the framework of PMIP3 (Paleoclimate Modelling Intercomparison Project, phase 3; see [8, Fig. 5.11]). Notably, the summer Middle Holocene response in the IAP RAS CM appeared to be considerably smaller than the respective response in the set of PMIP3 models.

The model-based results obtained in [9–11] indicate that the new geophysical phenomena (formation of craters in Yamal Peninsula) revealed in recent years can be explained by the increase in the near-surface temperatures in North Eurasia, in particular, on Yamal, with dissociation of relic gas hydrates that survived warming during the Holocene optimum. According to the estimates obtained at the simulation of scenarios of anthropogenic climate changes in the XXI century one can suggest a considerable increase in the risk of occurrence of similar phenomena in the Northern Hemisphere's [10]. It should be noted that the estimates depend on how well the modern models reproduce the climatic conditions of the Middle Holocene.

According to the simulations with IAP RAS CM, the average global precipitation is slightly

less (approximately by 5%) than the average precipitation estimated from GPCP-2.3 data (Global Precipitation Climatology Project, version 2.3; https://www.esrl.noaa.gov/psd/data/gridded/data.gpcp.html), and this is within the limits of estimate uncertainty from the modern data. Such uncertainty in reproducing precipitation is characteristic of the modern models for the Earth's system [12].

Based on the model calculations, the global area of natural fires generally increases through the Holocene due to the higher frequency of anthropogenic fires (Fig. 4). Remarkably, in the second quarter of the 20th century, areas of fires reduced considerably, and then increased from the mid-20th century. The model estimates of total areas of fires for recent decades are slightly higher than those according to the GFED-4 data (Global Fire Emission Database, version 4; https://www.globalfiredata.org/data.html). It should be noted that, among modern models of the Earth system, only a few include interactive blocks simulating dynamics of natural fires, and different models demonstrate significant scatter in their estimates of the areas of natural fires, at that [13].

Figure 4 also presents the changes in estimated areas of natural fires 6–4.5 kyr B.P. relative to the end of the 20th century (1971–1999). According to Fig. 4c, an increase in the area of natural fires in the Holocene is reported in most regions, excluding southern Eurasia. This generally agrees with the intensity of natural fires estimated from the data on charcoal deposits [14] and also with the calculations based on the CLIMBA Earth system model [15].

FUNDING

This work was conducted within the framework of the Russian Foundation for Basic Research, projects nos. 17–05–01097, 17–29–05098, 18–05–00087, 18–05–60111, and 18–45–160006, using the results obtained within the framework of the research program of the Russian Academy of Sciences ("Climate Changes: Causes, Risks, Consequences, Problems of Adaptation, and Regulation"). Comparative analysis of climatic regimes during the Holocene optimum and at present was supported by the Russian Science Foundation, project no. 19–17–00240.

REFERENCES

1. I. I. Mokhov and A. V. Eliseev, Dokl. Eath Sci. **443** (2), 532–536 (2012).
2. S. N. Denisov, A. V. Eliseev, I. I. Mokhov, et al., Izv., Atmos. Ocean. Phys. **51** (5), 482–487 (2015).
3. A. V. Eliseev, A. N. Ploskov, A. V. Chernokulsky, et al., Dokl. Eath Sci. **485** (1), 273–278 (2019).
4. A. V. Eliseev and I. I. Mokhov, Proc. SPIE **12208**, 1351–1361 (2019).
5. A. L. Berger, J. Atmos. Sci. **35** (12), 2362–2367 (1978).
6. J. Marsicek, B. N. Shuman, P. J. Bartlein, et al., Nature **554** (7690), 92–96 (2018).
7. Z. Liu, J. Zhu, Y. Rosenthal, et al., Proc. Natl. Acad. Sci. U. S. A. **111** (34), E3501–E3505 (2014).
8. *Climate Change 2013: The Physical Science Basis,* Ed. by T. Stocker, D. Qin, G. K. Plattner, (Cambridge Univ. Press, Cambridge, New York, 2007).
9. M. M. Arzhanov, I. I. Mokhov, and S. N. Denisov, Dokl. Eath Sci. **468** (2), 616–618 (2016).
10. M. M. Arzhanov and I. I. Mokhov, Dokl. Eath Sci. **476** (2), 1163–1167 (2017).
11. I. I. Mokhov, IOP Publ.: Earth Environ. Sci. **231**, 012037 (2019).
12. Z. Liu, A. Mehran, T. J. Phillips, et al., Clim. Res. **60** (1), 35–50 (2014).
13. S. Kloster and G. Lasslop, Global Planet. Change **150**, 58–69 (2017).
14. J. R. Marlon, R. Kelly, A.-L. Daniau, et al., Biogeosciences **13** (11), 3225–3244 (2016).
15. T. Brucher, V. Brovkin, S. Kloster, et al., Clim. Past **10** (2), 811–824 (2014).

Translated by N. Astafiev